

# Distortion of the p-mode peak profiles by the solar-cycle frequency shifts: do we need to worry?

W. J. Chaplin,<sup>1</sup> Y. Elsworth,<sup>1</sup> R. New,<sup>2</sup> and T. Toutain,<sup>1</sup>

<sup>1</sup> School of Physics and Astronomy, The University of Birmingham, Edgbaston, Birmingham B15 2TT, UK

<sup>2</sup> Faculty of Arts, Computing, Engineering and Sciences, Sheffield Hallam University, Sheffield S1 1WB, U.K.

2 February 2008

## ABSTRACT

We seek to address whether solar-cycle frequency shifts of the Sun’s low- $l$  p modes ‘distort’ the underlying shapes of the mode peaks, when those peaks are observed in power frequency spectra made from data spanning large fractions, or more, of the cycle period. We present analytical descriptions of the expected profiles, and validate the predictions through use of artificial seismic timeseries data, in which temporal variations of the oscillator frequencies are introduced. Our main finding is that for the Sun-like frequency shifts the distortion of the asymmetrical Lorentzian-like profiles is very small, but also just detectable. Our analysis indicates that by fitting modes to the usual Lorentzian-like models – which do not allow for the distortion – rather than new models we derive, there is a bias in the mode height and linewidth parameters that is comparable in size to the observational uncertainties given by multi-year datasets. Bias in the frequency parameter gives much less cause for worry, being over an order of magnitude smaller than the corresponding frequency uncertainties. The distortion discussed in this paper may need to be considered when multi-year Sun-like asteroseismic datasets are analyzed on stars showing strong activity cycles.

**Key words:** methods: data analysis – methods: statistical – Sun: helioseismology

## 1 INTRODUCTION

High-quality observations of the solar p modes are now available, which for some instruments cover almost three complete 11-yr cycles of activity (Chaplin et al. 2007a). Accurate and precise mode parameter data are a vital prerequisite for making accurate inference on the solar interior, be that on the hydrostatic or dynamic structure. There are clear advantages to be gained by extracting estimates of the mode parameters from power frequency spectra made from several, sometimes many, years of contiguous observations. The excellent resolution in frequency, and excellent height-to-background ratios observed in the mode peaks, then allows mode parameters to be extracted to extremely high precision. Subtle phenomena, such as asymmetry of mode peaks (a diagnostic of the stochastic excitation, and granulation) and asymmetry of mode frequency splittings (a diagnostic of the surface activity) may then also be extracted reliably from the data. And the weakly damped p modes at very low frequencies become visible and amenable to measurement and study.

The observations may then span a sizeable fraction, or more, of an 11-yr solar activity cycle period. The question arises: what effect do the well-known solar-cycle shifts in frequency through a long timeseries have on the underlying shapes of the mode peaks, when those peaks are observed in power frequency spectra made from the full timeseries? Are the shapes so *distorted* from

the Lorentzian-like form that the peak-bagging codes – with their Lorentzian-like fitting models – inevitably return biased estimates of the parameters? In this paper, we seek to answer this question for the low-degree (low- $l$ ) core-penetrating solar p modes. We seek an analytical description of the underlying peak-shapes expected from timeseries in which the frequencies of modes are known to vary. We then look at whether the form given is significantly different from the assumed Lorentzian-like profiles. We also use simulations of artificial timeseries data, in which temporal variations of the oscillator frequencies have been introduced, to validate use of the analytical expressions.

The frequency-shift regime of interest is illustrated in figure 1. The left-hand panel plots the sizes of the minimum-to-maximum solar-cycle frequency shifts of the low- $l$  modes (here, averaged over  $l = 0$  to 3), as a function of mode frequency (e.g., see Chaplin 2004). The average shift amounts to about  $0.4\,\mu\text{Hz}$  for a mode at  $\sim 3000\,\mu\text{Hz}$ . While modes at higher frequency suffer a bigger shift (e.g., about  $1\,\mu\text{Hz}$  at frequency  $4000\,\mu\text{Hz}$ ) their linewidths are then also about an order of magnitude larger than at  $3000\,\mu\text{Hz}$ , and it is the shift-to-linewidth ratio that is of relevance for determining the impact of any distortion. This ratio is plotted in the right-hand panel of figure 1: clearly, modes at the centre of the low- $l$  p-mode spectrum are potentially most susceptible to the distortion effect.

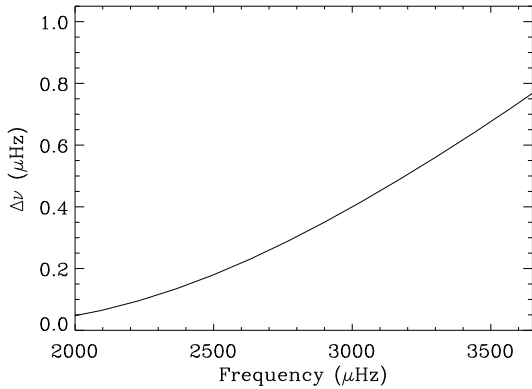


**Figure 1.** Left-hand panel: smoothed representation of the solar activity cycle frequency shifts (from minimum to maximum activity), averaged across  $l = 0$  to 3. Right-hand panel: Ratio of the shifts plotted in the left-hand panel and the linewidths of the modes.

## 2 MODEL OF MODE PROFILE FOR FREQUENCY-SHIFTED DATA

To obtain a model of the underlying profile of a p mode whose frequency is shifted in time, we note that the modes are excited and damped on a timescale much shorter than that on which any significant change of their frequency is observed. We therefore assume the resultant profile corresponds to the average of all the instantaneous profiles taken at any time  $t$  within the full period of observation  $T$ . We shall initially model the mode profiles as simple Lorentzians. Each instantaneous profile is therefore described as a Lorentzian with a central frequency  $\nu(t)$ , i.e., the ‘mode frequency’ at time  $t$ . The time-averaged profile is then

$$\langle P(\nu) \rangle = \frac{1}{T} \int_0^T \frac{H}{1 + \left(\frac{\nu - \nu(t)}{\Gamma/2}\right)^2} dt, \quad (1)$$

where the angled brackets indicate an average over time, and  $H$  and  $\Gamma$  are the mode height (maximum power spectral density) and linewidth, respectively.

In what follows we shall discuss the profiles given for two functions describing the frequency shifts in time: first, the simplest possible function, this being a linear variation over time; and second a sinusoidal variation to mimic the full solar activity cycle. We have neglected the effects of the solar-cycle variations in height and width, which will be included in future work.

## 3 ANALYTICAL MODE PROFILES

### 3.1 Linear variation in time

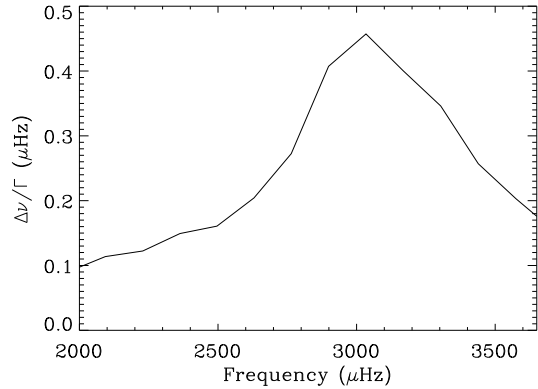
We begin by assuming a simple linear variation in time, i.e.,

$$\nu(t) = \nu_0 + \Delta\nu \frac{t}{T}, \quad (2)$$

where  $\nu_0$  is the unperturbed frequency, and the shift is calibrated so that the total shift from the start ( $t = 0$ ) to the end ( $t = T$ ) of the timeseries is  $\Delta\nu$ . Substitution of equation 2 into equation 1, followed by solution of the integral, gives the predicted mode profile:

$$\langle P(\nu) \rangle = \frac{H}{2\epsilon} \text{atan} \left( \frac{2\epsilon}{1 - \epsilon^2 + X^2} \right), \quad (3)$$

where



$$\epsilon = \frac{\Delta\nu}{\Gamma} \quad (4)$$

is the frequency shift in units of the mode linewidth and

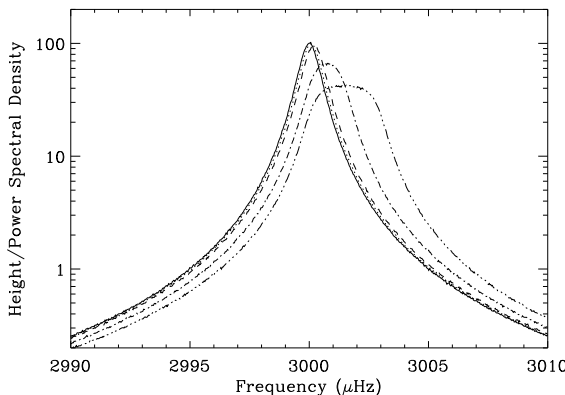
$$X = \frac{\nu - (\nu_0 + \Delta\nu/2)}{\Gamma/2}. \quad (5)$$

Figure 2 shows profiles given by equation 3. The unperturbed profile (solid line) is for a mode having an unperturbed frequency of  $\nu_0 = 3000 \mu\text{Hz}$ , an unperturbed linewidth of  $\Gamma = 1 \mu\text{Hz}$ , and an unperturbed height of  $H = 100$  units. The other curves show the profiles that result when the frequency shift,  $\Delta\nu$ , is: 0.15  $\mu\text{Hz}$  (dotted line); 0.40  $\mu\text{Hz}$  (dashed line); 1.50  $\mu\text{Hz}$  (dot-dashed line); and 3.0  $\mu\text{Hz}$  (dot-dot-dot-dashed line). Since  $\Gamma = 1 \mu\text{Hz}$ , the  $\Delta\nu$  also correspond to the shift-to-linewidth ratios,  $\epsilon$ . To put the values in context, low- $l$  modes at  $\approx 3000 \mu\text{Hz}$ , which also have width  $\approx 1 \mu\text{Hz}$ , suffer a total fractional shift of approximately 0.40  $\mu\text{Hz}$  from the minimum to the maximum of the solar activity cycle.

With reference to figure 2, it is evident that only at the two largest shifts (dot-dashed and dot-dot-dot-dashed lines) do the profiles depart appreciably from the Lorentzian form. However, these shifts are somewhat larger than those suffered by the real p modes. Closer inspection of the profiles does reveal some modest distortion at the two, smaller, Sun-like shifts. These have  $\epsilon = 0.15$  and 0.40 respectively. We discuss the implications of this distortion for introducing bias in results of the usual peak fitting in Section 5 below.

We also tested the predictions of equation 3 with Monte Carlo simulations of artificial data. The Laplace transform solution of the equation of a forced, damped harmonic oscillator was used to generate mode components at a 40-s cadence in the time domain, in the manner described by Chaplin et al. (1997). Components were re-excited independently at each sample with small ‘kicks’ drawn from a Gaussian distribution. The simulations gave modes having Lorentzian limit shapes in the power frequency spectrum. The underlying frequency of the oscillator was then varied over the course of the timeseries to give the required shifts. We averaged many thousands of independent realizations, for computations made at each of the shifts indicated above, to recover estimates of the underlying profiles that agreed excellently with the analytical predictions.

At first glance it would seem that the profile given by equation 3 is quite different from a Lorentzian. However, for  $\epsilon \ll 1$  the function simplifies to give a Lorentzian. In this case, by solving an



**Figure 2.** Peak profiles expected for a single mode of width  $1\,\mu\text{Hz}$  in the power frequency spectrum of a time series within which the frequency was varied in a linear manner by total amount  $\Delta\nu$ . Various linestyles are: no shift (solid line);  $\Delta\nu = 0.15\,\mu\text{Hz}$  (dotted line);  $0.40\,\mu\text{Hz}$  (dashed line);  $1.50\,\mu\text{Hz}$  (dot-dashed line); and  $3.0\,\mu\text{Hz}$  (dot-dot-dot-dashed line).

alytically the likelihood maximization of the profile described by equation 3, it is possible to show that  $H^*$  and  $\Gamma^*$ , the height and linewidth of this simplified (Lorentzian) function are, to the first non-null order, related to the original  $H$  and  $\Gamma$  by:

$$H^* = H \left(1 - \epsilon^2 \frac{\pi}{6W}\right), \quad (6)$$

and

$$\Gamma^* = \Gamma \left(1 + \epsilon^2 \frac{\pi}{6W}\right). \quad (7)$$

Here  $W$  is the width in frequency (in units of the linewidth  $\Gamma$ ) over which the fit is made in the power frequency spectrum. From these equations we can say that the linewidth will be slightly overestimated, and the height slightly underestimated, if a simple Lorentzian fitting model is used to fit the mode peaks. It is interesting to note that the estimates  $H^*$  and  $\Gamma^*$  tend towards  $H$  and  $\Gamma$  as  $W$  increases. This means that ideally with a sufficiently large frequency window it should be possible to recover the original parameters of the mode to good accuracy.

Finally in this section, we note that the observed solar low-*l* *p*-mode peaks are slightly asymmetric in shape, albeit at the level of only a few per cent at most. It is also possible to derive a version of equation 3 based on an unperturbed profile that is asymmetric, e.g., based on the widely-used asymmetric formalism of Nigam & Kosovichev (1998). The profile that is given is:

$$\langle P(\nu) \rangle = \frac{H}{2\epsilon} \text{atan} \left( \frac{2\epsilon}{1-\epsilon^2+X^2} \right) \quad (8)$$

$$+ B \frac{H}{2\epsilon} \log \left( \frac{1+(X+\epsilon)^2}{1+(X-\epsilon)^2} \right), \quad (9)$$

where  $B$  is the peak asymmetry parameter. In the limit of small frequency shifts we then have

$$\langle P(\nu) \rangle = \frac{H}{1-\epsilon^2+X^2} \left[ 1 + 2BX \left( 1 + \epsilon^2 \eta(X, \epsilon) \right) \right], \quad (10)$$

with  $\eta$  a function of  $X$  and  $\epsilon$  that satisfies  $|\eta(X, \epsilon)| \leq 1$ . Equation 10 shows that the usual Nigam-Kosovichev profile still holds. However, as for the height and the linewidth parameters the asymmetry will be changed by a small amount, this amount being proportional to  $\epsilon^2$ .

### 3.2 Cosinusoidal variation in time

The linear model above is useful for representing observations made on the steepest parts of the rising or falling phases of the solar activity cycle, where the global activity varies approximately linearly in time. But what if the observations also cover the other, non-linear parts? We therefore also consider the following time dependence for the mode frequency

$$\nu(t) = \nu_0 + \frac{\Delta\nu}{2} \left[ 1 - \cos \left( \frac{2\pi t}{P_{\text{cyc}}} \right) \right], \quad (11)$$

because it mimics the ‘periodic’ pattern of the solar activity cycle. The variation is formulated as shown above so that  $\nu_0$  is again the unperturbed frequency (i.e., the frequency at minimum activity); while  $\Delta\nu$  is now the full amplitude (from minimum to maximum) of the cyclic frequency shift (not the *total* shift, as in the linear model). When the length of observation,  $T$ , equals the cycle period  $P_{\text{cyc}}$  (or one-half of the period) it can be shown that the average profile resulting from equation 11 is:

$$\langle P(\nu) \rangle = \frac{\sqrt{L_1 L_2}}{\sqrt{1 - \epsilon^2 F(L_1, L_2)}}, \quad (12)$$

where

$$\begin{aligned} F(L_1, L_2) &= \frac{4L_1 L_2}{H \left( \sqrt{L_1} + \sqrt{L_2} \right)^2}, \\ L_1 &= \frac{H}{1 + (X - \epsilon)^2}, \\ L_2 &= \frac{H}{1 + (X + \epsilon)^2}, \\ X &= \frac{\nu - (\nu_0 + \frac{\Delta\nu}{2})}{\Gamma/2}, \\ \epsilon &= \frac{\Delta\nu}{\Gamma}. \end{aligned}$$

In this case it is interesting to note that since the frequency spends more time around its maximum and minimum values, power near these extreme frequencies will have more weight in the time-averaged profile, giving the profile a double-humped appearance. This is reflected in the profile analytical expression through the two Lorentzians  $L_1$  and  $L_2$ . It is obvious from equation 12 that when  $\epsilon \ll 1$  the profile tends to a single Lorentzian.

Figure 3 shows predicted profiles from equation 12, assuming observations made over a complete activity cycle, and with the same shifts  $\Delta\nu$  that were applied in the linear-model case (see figure 2 and Section 3.1). These profiles have again been validated by averaging many independent power frequency spectrum realizations made from stochastic harmonic oscillator timeseries. As for the simpler linear variation, it is only at the two largest  $\Delta\nu$  that the profiles depart appreciably from the unperturbed (Lorentzian) form, here showing the predicted ‘humps’ at the extreme frequencies of the cycle. However, closer inspection again reveals some minimal distortion of the Lorentzian shapes at the small Sun-like shifts. For a given shift, this distortion appears to be slightly larger than in the simpler, linear case. The implications of this distortion for parameter bias are discussed in Section 5 below.

As in the case of a linear frequency shift it is also possible to derive a version of equation 12 based on an unperturbed profile that is asymmetric in shape. The profile that is given is:

$$\langle P(\nu) \rangle = \frac{\sqrt{L_1 L_2}}{\sqrt{1 - \epsilon^2 F(L_1, L_2)}} \left[ 1 + 2BX \left( 1 - \epsilon^2 F(L_1, L_2) \right) \right], \quad (13)$$

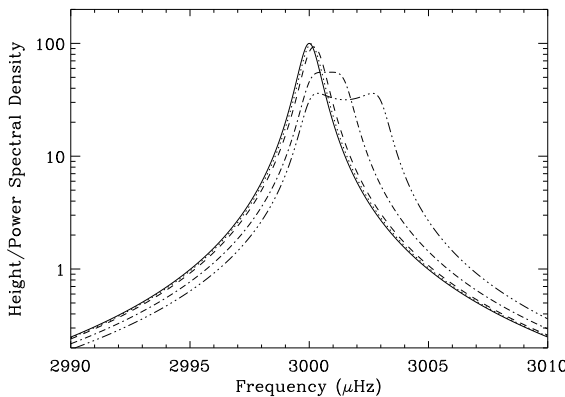


**Figure 3.** Peak profiles expected for a single mode of width  $1\,\mu\text{Hz}$  in the power frequency spectrum of a time series within which the frequency was varied in a cosinusoidal manner. The timeseries is assumed to have length equal to one cycle period; while the amplitude of the cycle is  $\Delta\nu/2$  (giving a total minimum-to-maximum shift in frequency of  $\Delta\nu$ ). Various line styles are: no shift (solid line);  $\Delta\nu = 0.15\,\mu\text{Hz}$  (dotted line);  $0.40\,\mu\text{Hz}$  (dashed line);  $1.50\,\mu\text{Hz}$  (dot-dashed line); and  $3.0\,\mu\text{Hz}$  (dot-dot-dashed line). Note that only at the two largest shifts do the profiles depart significantly from the unperturbed (Lorentzian) profile.

where  $B$  is again the peak asymmetry parameter.

#### 4 ESTIMATION OF FREQUENCY SHIFT USING NEW FORMALISM

Solar-cycle frequency shifts of  $p$  modes are usually estimated by extracting estimates of mode frequencies from short timeseries, distributed at different epochs along the solar activity cycle. In this section, our aim is to see whether it is instead possible to use the new analytical expressions to extract estimates of the frequency shifts. The observed time variations of the mode frequencies have a qualitatively similar form to the cosinusoidal time variation on which equations 12 and 13 are based (e.g., see Chaplin et al. 2007a). The idea is that by using the new equations to model the mode peaks in the peak-bagging codes it may be possible to estimate the frequency shifts, since those shifts may give rise to measurable distortions.

In our tests we assume the observations span approximately one complete solar activity cycle, and so we therefore use fitting models based on the cosinusoidal model. A cosinusoidal variation is of course not an ideal match to the real observed time variation of the solar activity cycle; however, our point here is to test the principle of the technique. We begin with tests on artificial data that do have an underlying variation of the frequencies that is cosinusoidal in time. We then apply the technique to real low- $l$  timeseries, which have lengths spanning approximately one 11-yr solar activity cycle.

##### 4.1 Application to artificial data

We first made 1000 realizations of an artificial timeseries comprising an  $l = 0/2$  mode pair, in which the modes were given underlying parameters expected for low- $l$  modes at  $\sim 3000\,\mu\text{Hz}$ . Frequencies of the artificial modes were varied over time in a cosinusoidal manner. The timeseries were each  $T = 11$  yr long – corresponding to the length of the artificial cycle,  $P_{\text{cyc}}$  – and all modes were given a total frequency shift, from the minimum to the maximum of the cycle, of  $\Delta\nu = 0.4\,\mu\text{Hz}$ . The artificial mode pairs were then fitted in

power frequency spectra of the timeseries to fitting models based on equation 13. The results showed it was possible to extract estimates of the frequency shift given to the modes, to a typical precision of  $\sim 0.15\,\mu\text{Hz}$ .

In 50 cases out of the total of 1000 simulations (i.e., in 5 per cent of the realizations) the fits ‘locked onto’ a null, or zero-valued, estimate of the frequency shift. This is a recurrent problem when fits are made for parameters which are too sensitive to the realization noise (e.g., estimation of component frequency splittings of blended modes). In such cases the maximum of the likelihood function can be far enough from the solution that it lies outside the range accessible to the parameter. The fit is therefore ‘stopped’ by the hard limit, which is zero in the case of the frequency shift.

As noted in Section 4 above, the classic approach to estimation of the shifts involves dividing the full timeseries into shorter subseries, which are then fitted to yield time-dependent estimates of the frequencies. Analysis of the resulting set of frequency estimates yields an estimate of the total frequency shift. When we applied this classic approach to the 1000 artificial timeseries, we found it was possible to estimate the shift to a precision of  $\sim 0.07\,\mu\text{Hz}$ . The precision is clearly superior to that given by fitting the new equations to the peak profiles. This is not surprising: We showed in Section 3.2 that for realistic low- $l$  frequency shifts the distortion of the mode profiles is very modest. This makes it hard to measure the distortion, and extract a robust estimate of the frequency shift, using the new technique.

We then extended the Monte-Carlo tests to simulate a range of mode pairs across the low- $l$  power frequency spectrum. We adopted the strategy of Toutain, Elsworth & Chaplin (2005), whereby the artificial underlying limit power frequency spectrum was computed and then fitted. This strategy saves on computing time, since one does not have to generate, and then fit, a large number of independent timeseries to give useable statistics. Equation 13 was used to make the mode profiles. The best-fitting uncertainties on fits made to these artificial data gave direct estimates of the precision expected from a single timeseries realization of the same length as that used to compute the underlying limit power frequency spectrum. (Note the fits recover the input bias accurately, since the fitting model was based on the equations that were used to describe the artificial profiles.) The results, which are plotted in figure 4, show that the precision in the estimates is quite modest, particularly at lower frequencies where the input frequency shifts are smallest in size.

##### 4.2 Application to real data

Next, we made use of four timeseries of real disc-integrated Doppler velocity observations of the Sun. Two timeseries comprised Sun-as-a-star observations: one made of data collected by the ground-based BiSON between 1993 and 2003; and one made of data collected by the GOLF instrument on board the *ESA/NASA SOHO* spacecraft between 1996 and 2004. The other two timeseries comprised resolved-Sun observations that were spatially averaged to give a Sun-as-a-star proxy signal: one made of data collected by the ground-based GONG between 1995 and 2004; and one made of data collected by the MDI instrument on SOHO between 1996 and 2006. Each of the four timeseries covers more or less one 11-yr cycle of solar activity.

The power frequency spectrum of each timeseries was computed, and low- $l$  mode pairs were fitted to models based on equation 13. We used equation 13, rather than equation 12, because the real low- $l$  peaks show small amounts of asymmetry. The  $l = 0/2$

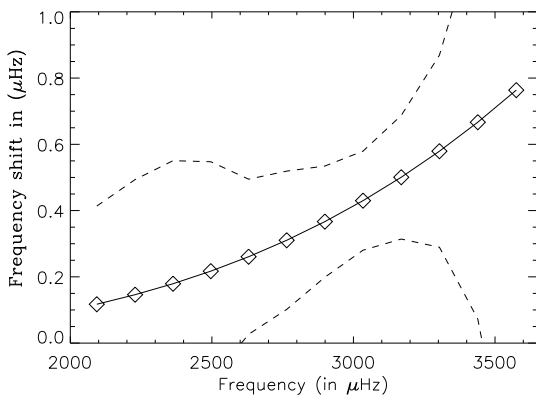


**Figure 4.** Fitted frequency shifts (symbols, with associated  $1\sigma$  error envelope shown by dashed lines) and input frequency shifts (solid line) for modes in artificial  $l = 0/2$  mode pairs. The frequency shifts were estimated by fitting the artificial mode peaks to fitting models based on equation 13.

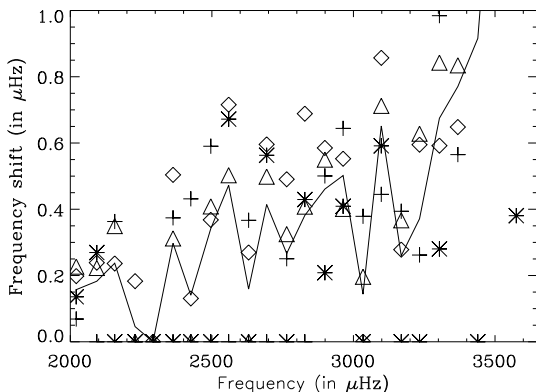


**Figure 5.** Estimated frequency shifts, averaged over  $l = 0, 1$  and 2 modes, as extracted from fits to BiSON (stars), MDI (crosses) GONG (diamonds) and GOLF (triangles) power frequency spectra. The solid line is an average of all four sets of frequency shifts. The frequency shifts were estimated by fitting the artificial mode peaks to fitting models based on equation 13.

pairs were fitted assuming all constituent components had the same frequency shift. For the  $l = 1/3$  pairs, our fitting results demonstrated that the relative weakness of the  $l = 3$  peaks meant the distortion of their profiles could not be fitted reliably. At  $l = 1$ , the blending of the constituent components of each mode caused some problems for the fitting, which was manifested by cross-talk between the fitted frequency shift and frequency splitting parameters.

Figure 5 shows the estimated frequency shifts as a function of mode frequency, averaged over  $l = 0, 1$  and 2 for each timeseries (see caption). As we would have expected, given the simulation results discussed in the previous section, it was not always possible to extract accurate estimates of the frequency shifts, and there were therefore several occasions on which the fits locked onto zero-valued estimates. Nevertheless the non-zero best-fitting values follow the expected trend in frequency, giving estimates of the shifts that are consistent with previous frequency-dependent estimates for the low- $l$  modes (e.g., Chaplin et al. 2001; Jiménez-Reyes et al. 2001; Gelly et al. 2002), apart from the highest frequencies, where the shifts are somewhat larger.

## 5 BIAS ON MODE PARAMETERS

In the previous sections we have seen that mode peaks of the low- $l$  solar  $p$  modes should be slightly distorted, with respect to the basic Lorentzian-like profiles, when they are observed in power frequency spectra made from observations spanning a substantial fraction or more of the 11-yr solar activity cycle. This distortion is caused by variation of the mode frequencies over time. Even though the distortion is modest we have demonstrated that it is possible to measure the distortion (and estimate frequency shifts) by using new fitting models.

This result raises an important question: if the mode profiles are indeed distorted, what bias might we expect in the best-fitting mode parameters were we to continue to use the (inaccurate) Lorentzian-like fitting models (e.g., the asymmetric Nigam-Kosovichev formalism)? We use results on artificial (Section 4.1) and real (Section 4.2) solar  $p$ -mode data to seek an answer to this question.

Let us consider first results on artificial data. We again adopted the strategy of Toutain, Elsworth & Chaplin (2005), creating artificial underlying limit power frequency spectra corresponding to 11-yr of observations. Equation 13 was used to make the mode profiles, with the assumed input frequency shifts having the same sizes as those shown in figure 4. The low- $l$  pairs were then fitted to fitting models made with the Nigam-Kosovichev formalism. Comparison of the fitted and input parameters gave the bias estimates plotted as solid lines in the left-hand (for linewidth) and right-hand (for frequency) panels of figure 6.

The dotted line in the left-hand panel shows the full best-fitting linewidth uncertainty (which is of similar magnitude to the height uncertainty). The overestimation of the linewidth – a similar-sized underestimation of the height is also observed – is seen to be of a size comparable to the estimated uncertainties. The dotted line in the right-hand panel is one-tenth the size of the best-fitting mode frequency uncertainty. Bias in the mode frequencies is evidently very small indeed, in contrast to the linewidth parameter. That said, we need to interpret the frequency result with a little care.

When the observations span either a complete cycle (as here), or one half of a cycle, the frequency parameter should in principle not be biased because the distortion is symmetric in frequency. Evidently, the small residual bias exhibited in the right-hand panel of figure 6 is due to other effects (e.g., from parameter cross-talk in the fitting, and the impact of the asymmetric shapes of the peaks). We would, however, expect there to be a bias from the distortion effect when observations span, say, one-quarter of a cycle. Under these circumstances the distortion will not be symmetric in frequency.

To test this case, and other intermediate cases, we made further artificial datasets. Artificial power frequency spectra were made to mimic observations ranging in length from 1 to 11 yr. Furthermore, the observations were assumed to start anywhere from the beginning of the activity cycle up to year 10 of the cycle (in 1 yr steps). Estimates of the frequency bias of modes at  $3000\text{ }\mu\text{Hz}$ , as a function of the simulated length of the observations, are plotted in figure 7. The various curves show the bias – as a percentage of the formal frequency uncertainty – for different starting points along the 11-yr cycle. The magnitude of the bias never rises above a few per cent of the frequency uncertainty. We may therefore conclude that frequency bias is not a major cause for concern.

Next, we fitted low- $l$  modes in the BiSON, GOLF, GONG and MDI power frequency spectra (Section 4.2) to fitting models made with the Nigam-Kosovichev formalism. By taking differences between these results and those from fits to models based on equa-

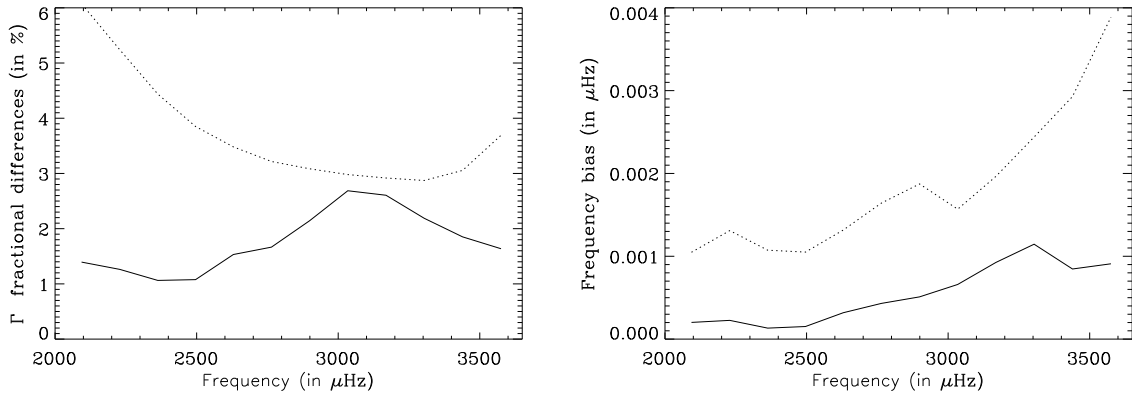


**Figure 6.** Expected linewidth (left-hand panel) and frequency (right-hand panel) parameter bias given by fitting the usual asymmetric Lorentzian-like fitting models to the mode peaks, models which do not account for the distortion of the underlying profiles. The dotted line in the left-hand panel shows the full best-fitting linewidth uncertainty. The dotted line in the right-hand panel is one tenth the size of the formal frequency uncertainty.

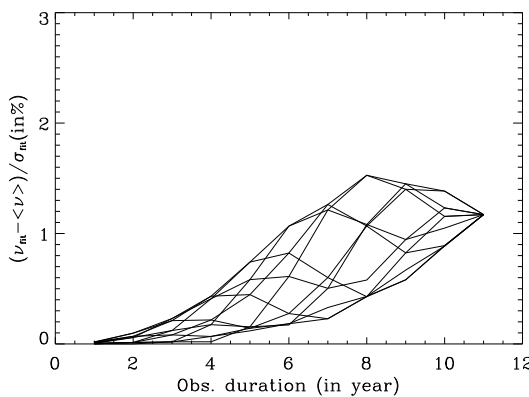


**Figure 7.** Estimated frequency bias (from simulations) for modes at  $3000\mu\text{Hz}$ . The bias is plotted in units of the formal frequency uncertainties as a function of the length of the observations. Each of the curves show results for different starting points along the simulated 11-yr solar activity cycle.

tion 13 we had another means of judging the bias. The results (symbols for different timeseries) are shown in the two panels of figure 8. The solid line in the left-hand panel shows the full best-fitting linewidth uncertainty; while the solid lines in the right-hand panel correspond to plus and minus one-tenth of the formal frequency uncertainty.

The results are shown to be in reasonable agreement with those of the artificial data (figure 6). Overestimation of the linewidths (left-hand panel of figure 8) is on average larger than the overestimation implied by the results of the simulations. We believe this largely reflects the fact that in the real data it is not only the frequencies that vary over the solar cycle, but also the heights, linewidths (e.g., Chaplin et al. 2000) and peak asymmetries (Jiménez-Reyes et al. 2007). In deriving the equations (e.g., equation 13), and constructing the artificial data for the simulations, we assumed only the frequencies varied in time. Proper allowance will be made for the height, linewidth and asymmetry variations in the next phase of this work.

Bias in the frequencies (right-hand panel of figure 8) is again

shown to be but a small fraction of the size of the frequency uncertainties.

## 6 CONCLUSION

We have studied the impact of the solar-cycle frequency shifts on the underlying shapes of p-mode peaks seen in power frequency spectra made from data spanning large fractions of the cycle period. Analytical descriptions of the resulting mode profiles were presented for two functions describing the shifts in time: a simple linear variation; and a sinusoidal variation to mimic the full solar activity cycle.

We presented plots of the profiles expected for shifts similar in size to, and also larger than, those observed for the low- $l$  solar p modes. The analytical predictions were also validated by Monte Carlo simulations with artificial data. In summary, we showed that while any distortion of the Lorentzian-like profiles of the solar p modes is very modest, it is nevertheless just detectable. Furthermore our analysis indicates that by fitting modes to the usual Lorentzian-like models – which do not allow for the distortion – rather than new models we derive, overestimation (underestimation) of the linewidth (height) parameter results. This bias is estimated to be of size comparable to the observational uncertainties given by datasets of length several years. Bias in the frequency parameter is much less of an issue, being over an order of magnitude smaller than the frequency uncertainties.

The distortion discussed in this paper may of course be an issue for analysis of multi-year asteroseismic datasets on some stars that show Sun-like oscillations. The effect will be most important in those stars for which the ratio of the stellar-cycle frequency shifts to the mode linewidths is larger than for the Sun. Indeed, visible distortion of the mode profiles in asteroseismic data may provide an initial diagnostic of strong stellar-cycle signatures over the duration of the observations (Chaplin et al. 2007b; Metcalfe et al. 2007).

We finish by offering an answer to the question posed by the title of this paper. As far as the low- $l$  solar p-mode frequencies are concerned, there is probably no need to worry about the distortion introduced by the frequency-shift effect. However, in the case of the height and linewidth parameters, a systematic bias of  $1\sigma$  or more means we do need to worry if we wish to obtain accurate estimates of these parameters.

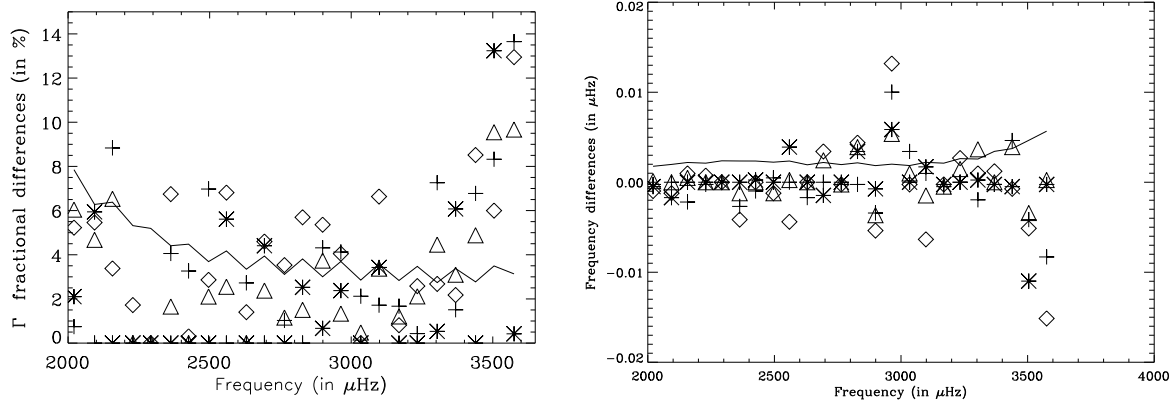


**Figure 8.** Differences between results of fitting power frequency spectra with fitting models based on the Lorentzian-like Nigam & Kosovichev model and equation 13. The left-hand panel shows linewidth differences, the right-hand panel frequency differences (averaged over  $l = 0, 1$  and 2 modes) in BiSON (stars), MDI (crosses) GONG (diamonds) and GOLF (triangles) frequency power spectra. The solid line in the left-hand panel shows the typical best-fitting linewidth uncertainty; while the solid lines in the right-hand panel correspond to plus and minus one-tenth of the typical formal frequency uncertainty.

## ACKNOWLEDGMENTS

BiSON is funded by the UK Science and Technology Facilities Council (STFC). We would like to thank all those who are, or have been, involved in BiSON. GOLF and MDI and are the result of the cooperative endeavours of several institutes, to whom we are deeply indebted. SOHO is a mission of international co-operation between *ESA* and *NASA*. This work also utilizes data obtained by the Global Oscillation Network Group (GONG) Program, managed by the National Solar Observatory, which is operated by AURA, Inc. under a cooperative agreement with the National Science Foundation. The data were acquired by instruments operated by the Big Bear Solar Observatory, High Altitude Observatory, Learmonth Solar Observatory, Udaipur Solar Observatory, Instituto de Astrofísica de Canarias, and Cerro Tololo Inter-American Observatory. The authors acknowledge the support of STFC.

## REFERENCES

Chaplin, W. J., Elsworth, Y., Isaak, G. R., McLeod, C. P., Miller, B. A., New, R., 1997, MNRAS, 287, 51  
 Chaplin, W. J., Elsworth, Y., Isaak, G. R., Miller, B. A., New, R., 2000, MNRAS, 313, 32  
 Chaplin, W. J., Appourchaux, T., Elsworth, Y., Isaak, G. R., New, R., 2001, MNRAS, 324, 910  
 Chaplin, W. J., Elsworth, Y., Isaak, G. R., Miller, B. A., & New, R., 2004, MNRAS, 352, 1102  
 Chaplin, W. J., Elsworth, Y., Miller, B. A., New, R., Verner, G. A., 2007a, ApJ, 659, 1749  
 Chaplin, W. J., Houdek G., Elsworth, Y., New, R., 2007b, MNRAS, 377, 17  
 Gelly B., et al., 2002, A&A, 394, 285  
 Jiménez-Reyes, S. J., Corbard, T., Pallé, P. L., Roca Cortés, T., Tomczyk S., 2001, A&A, 379, 622  
 Jiménez-Reyes, S. J., Chaplin, W. J., Elsworth, Y., Garcia, R. A., Howe, R., Socas-Navarro, H., Toutain, T., 2007, ApJ 654, 1135  
 Metcalfe T. S., Dziembowski W. A., Judge P. G., Snow M., 2007, MNRAS, 379, L16  
 Nigam, R. & Kosovichev, A. G., 1998, ApJ, 505, L51  
 Toutain, T., Elsworth, Y., Chaplin, W. J., 2005, A&A, 433, 713